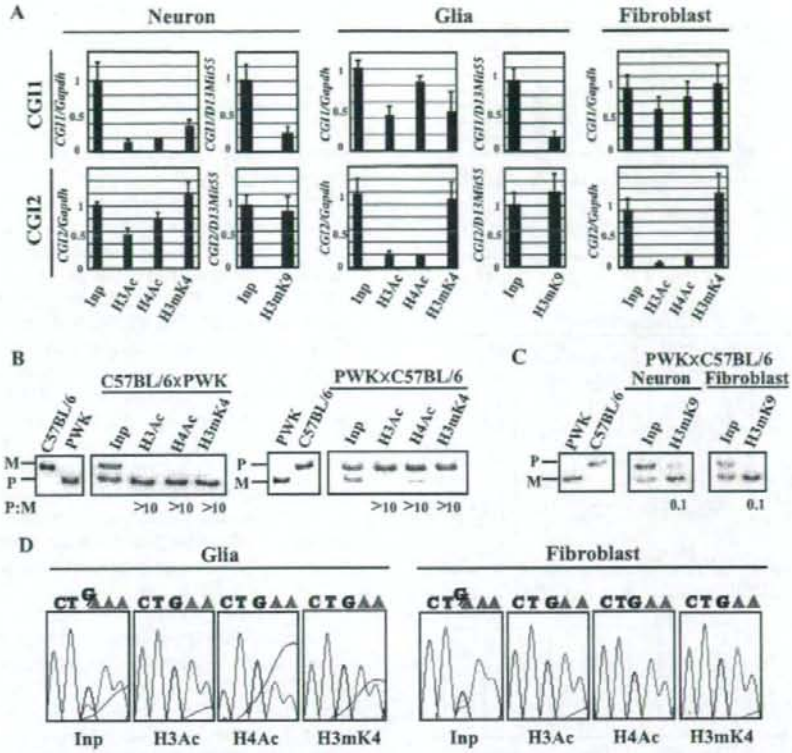

FIG. 5. Histone modification analysis of the *Grb10* promoter in cultured cells. (A) Quantitative analysis of immunoprecipitated DNA by real-time PCR. Quantitative values of precipitated DNA in CGI1 and CGI2 were normalized by dividing the average value of each CGI by the average value of *Gapdh* or *D13Mit55*. Standard errors of the means are indicated by bars. (B) Allele-specific histone modifications in CGI2 in neurons by hot-stop PCR. Digested PCR products of C57BL/6 and PWK genomic DNA are shown as homozygous controls in the first two lanes. M and P represent the products from the maternal allele and the paternal allele, respectively. The ratio of the paternal to maternal (P:M) band intensities, corrected by the ratio in input chromatin (Inp), is indicated below each lane. (C) Allele-specific histone H3K9 methylation in CGI2 by SSCP. PCR products of C57BL/6 and PWK genomic DNA were shown as controls in the first two lanes. (D) Allele-specific histone modifications in CGI1 by sequence chromatograms. Glial cells and fibroblasts derived from F_1 hybrids [(C57BL/6 × PWK)F_1] were used for analysis. The single-nucleotide (G/A) polymorphism is detected in the input sample (Inp); "G" originated from the maternal allele and "A" from the paternal allele.

results in vitro can explain the previous data that the brain type transcript was not detected in whole embryo at E9.5 (17), when neurogenesis has not yet occurred. In addition, our data on *Grb10* expression, i.e., brain development-dependent switching from the major-type to the brain type transcript, can also support the previous report that *Grb10* is expressed predominantly from the paternal allele in the adult brain (17), which consists of neurons and glial cells.

In our expression analysis, we detected both brain type and major-type transcripts in cultured neurons (Fig. 2B). Recently, it was reported that the *Pcdh* (protocadherin) gene was monoallelically expressed in individual neurons (10). The *Pcdh* gene family (*Pcdha*, *Pcdhb*, and *Pcdhc*) has variable exons and alternative splice forms. Esumi et al. analyzed the expression of transcripts in the variable exons of *Pcdha* by using a single-cell RT-PCR approach for the determination of the allelic origin for each variable exon at the individual cell level (10). The individual cells showed monoallelic expression for each variable exon. In our analysis of *Grb10*, the discrepancy between the modifications in CGI1 and the expression of the major-type transcript in neurons was recognized. Similar to a monoallelic expression pattern of variable *Pcdha* exons in individual neurons, the discrepancy may be explained by the existence of two different cell populations in cultured neurons, each of which expresses either the major-type or the brain type transcript exclusively. As shown in Fig. 2D, the brain type transcript was obviously highly expressed compared to the major-type transcript during long culture periods. The larger population of cells with the brain type transcript may affect the result of histone modifications more than the smaller population of cells with the major-type transcript.

It has been reported that histone modifications and DNA methylation are not synchronized as a transcriptionally active/silent signal in some imprinted genes, such as *NDN*, *Gnas*, and

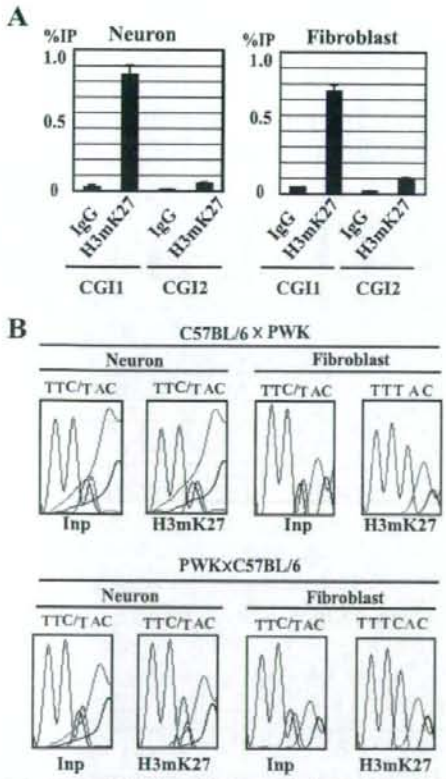

FIG. 6. Histone H3K27 methylation analysis of CGI1 and CGI2 in cultured cells. (A) Quantitative analysis of immunoprecipitated DNA by real-time PCR. The percentage of immunoprecipitation (IP) was calculated by dividing the quantitative value of precipitated DNA by that of the corresponding input DNA. Standard errors of the means are indicated by bars. (B) Allele-specific histone modifications in CGI1 by sequence chromatograms. Neurons and fibroblasts derived from F_1 hybrids (C57BL/6 × PWK; PWK × C57BL/6) were used for analysis. The single-nucleotide (C/T) polymorphism is detected in the input sample (Inp); "C" originated from the C57BL/6 allele and "T" from the PWK allele. IgG, immunoglobulin G.

Igf2r (21, 22, 23, 33, 35). Our data also showed an epigenetically unsynchronized active/silent signal between DNA methylation and histone modifications in *Grb10* (Fig. 7). In this study, we showed that the brain type transcript is expressed in neurons but not in glial cells (Fig. 2C), where both differential methylation in CGI2 and biallelic hypomethylation in CGI1 were maintained regardless of expression (Fig. 4B). The result that allele-specific DNA methylation is not sufficient to direct imprinted expression in brain cells implies that other epigenetic modifications may affect cell lineage-specific imprinting.

In our analysis of histone modifications, histone acetylation status correlated with the expression status of the major-type transcript in glial cells and fibroblasts and the brain type transcript in neurons (Fig. 7). Such histone acetylation status in *Grb10* expression is consistent with the findings that allele-specific histone acetylation was associated with allelic gene expression in the imprinted gene, *NDN* (21). Histone acetylation offers the best example of a direct link between tissue-specific gene expression and histone modifications.

Unlike that of histone acetylation, the status of histone methylation has been implicated as an early event for chromatin conformations. Methylation of histones H3K4 and H3K9 is associated with active chromatin and silent chromatin, respectively. According to our results, allele-specific H3K4 and H3K9 methylation in CGI1 and CGI2 did not correlate with allele-specific gene expression in each cultured cell. In glial cells, H3K4 in CGI2 was hypermethylated in the paternal chromosome, which was silent with no brain type transcript. It seems that H3mK4 is maintained during differentiation as an imprint mark with H3mK9 but is not related to promoter activity (28), although histone modifications in oocytes remain unknown. In CGI1, H3me2K9 and H3me3K9 were hypomethylated in both parental chromosomes independent of the expression of the major-type transcript in cultured cells. It is likely that H3K9 methylation in germ cells is maintained as a stable and heritable imprint mark but may not be secondarily acquired during development.

Then, how is maternal chromosome-specific expression of the major-type transcript regulated without differential DNA methylation in CGI1? The PcG protein Eed complex is known to be a part of a memory system that maintains repression of

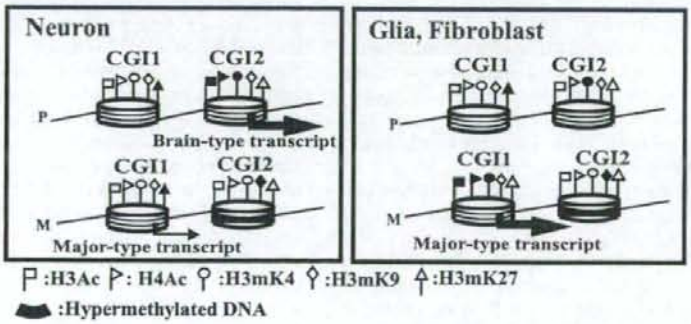

FIG. 7. Summary of epigenetic modifications across promoter regions of *Grb10*. M and P represent maternal and paternal chromosomes, respectively. Large and small arrows indicate expression levels. The nucleosome model shows DNA wrapping around a histone octamer with some histone modifications. White and black flags represent hypoacetylated/hypomethylated and hyperacetylated/hypermethylated statuses, respectively.

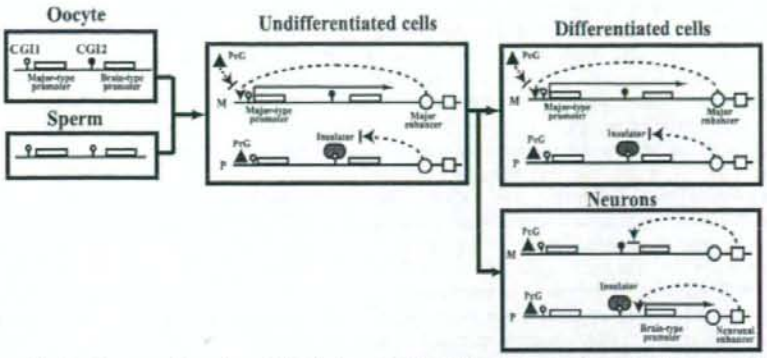

FIG. 8. Working models for tissue-specific reciprocal imprinting of *Grb10*. The previous enhancer/insulator model by Hikichi et al. was modified based on the analysis of DNA methylation and histone modifications mediated by the PcG complex containing Eed (17). Tissue-specific imprinting of *Grb10* implies neuron-specific imprinting that is different from imprinting in other undifferentiated and differentiated cells. Black and white lollipops indicate hypermethylated and hypomethylated DNA, respectively. Circles and squares indicate putative major enhancer and neuronal enhancer, respectively, which accelerate *Grb10* expression from the major-type promoter and the brain type promoter, respectively. The PcG complex containing Eed is represented by a triangle. CTCF is thought to be a putative insulator (gray oval). M, maternal; P, paternal.

the imprinted X chromosome (36) and silencing of some imprinted genes (24, 33). *Grb10* is reported to be one of the imprinted genes that are regulated by the PcG protein Eed complex. Interestingly, in $Eed^{-/-}$ embryos, the major-type transcript was biallelically expressed without major alteration of allelic DNA methylation (24). The Eed/Ezh2 PcG complex possesses histone methyltransferase activity on H3K27 (5, 8, 25) and interacts with histone deacetylases (34). Methylation of H3K27 is a repressive epigenetic mark regulated by the SET domain containing Ezh2/Eed complex (5, 8, 20, 25). In our analysis, H3mK27 was clearly precipitated in neurons and fibroblasts in CGI1 but not in CGI2 (Fig. 6A). The paternal chromosome-specific methylation of H3K27 in CGI1 was observed in fibroblasts but not in neurons (Fig. 6B). These data indicate that the Eed PcG complex can biallelically interact on CGI1 as a *trans*-acting factor in neurons but paternally in other cells. In the absence of DNA methylation in CGI1, PcG complexes may mediate a nonpermissive chromatin state for transcription, leading to repressive histone modifications. Interestingly, other genes, *Cdkn1c* and *Ascl2*, imprinting of which was reported to be regulated by Eed (24), show tissue-specific imprinting, and their imprinted expression in trophoblasts is associated with repressive histone H3K27 methylation rather than DNA methylation (22, 33).

Figure 7 shows the summary of our data. In CGI2, DNA methylation in a gametically methylated CpG island on the maternal allele was maintained throughout development. Allelic methylation of H3K4 and H3K9 associated with gametic DNA methylation was also stable as an epigenetic mark, independent of *Grb10* expression. Histone acetylation status was correlated with the expression status of the brain type transcript: histones H3 and H4 were paternally acetylated only in neurons, where the brain type transcript was paternally expressed. H3K27 was not methylated biallelically. In CGI1, biallelic DNA hypomethylation and biallelic hypomethylation of H3K9 were observed. Acetylation of histones H3 and H4 and methylation of H3K4 and H3K27 were allelically detected, corresponding to the allelic expression of the major-type transcript, although the discordance in histone modifications and expression in neurons was detected, probably depending on maturation of neurons. Methylation of H3K9 and H3K27 is thought to be a repressive chromatin marker, but it is not completely clear whether PcG-mediated silencing involves methylation of H3K9 synchronized with H3mK27 in all PcG target genes. We did not observe coexistence of H3mK27 and H3mK9 in both CGI1 and CGI2 of *Grb10*. Umlauf et al. also reported discordance between localizations of H3mK27 and H3mK9 in some imprinted genes in the *Kcnq1* domain (33). Further work should determine how histone modifications, especially methylation of H3K9 and H3K27, are coordinated or uncoordinated as epigenetic determinants in tissue-specific imprinting.

These data about epigenetic modifications analyzed at the cell level, in addition to the evidence for $Dnmt3L^{m-/-}$ and $Eed^{-/-}$ embryos, lead to a working model for tissue-specific reciprocal imprinting of *Grb10* (Fig. 8). The previous model by Hikichi et al. (17) was modified in our model based on the data of DNA methylation and repressive histone modifications mediated by the PcG complex in brain cell lineages. In undifferentiated cells, a DNA methylation-sensitive insulator, CTCF, binds to the paternal CGI2 and blocks the paternal activity of the downstream major enhancer, resulting in silent expression of the major-type transcript on the paternal allele. On the maternal allele, the major enhancer works on the major-type promoter to recruit transcription factors. In CGI1, the Eed/Ezh2 PcG complex binds on the paternal allele, whereas it competes with transcription factors on the maternal allele. The Eed/Ezh2 PcG complex methylates H3K27 and interacts with histone deacetylases, leading to silencing of the chromatin on the paternal CGI1. In $Dnmt3L^{m-/-}$ embryos, biallelic hypomethylation in CGI2 makes CTCF bind biallelically on CGI2, resulting in null expression of the major-type transcript, regardless of the PcG complex. In $Eed^{-/-}$ embryos, the silent state on the paternal CGI1 regulated by the Eed PcG complex

is released to the biallelically active state without major alteration of DNA methylation in maternal CGI2. In neurons, the other molecular mechanism of imprinting works in a promoter-specific manner, different from that in other differentiated cells. During neurogenesis, expression of *Grb10* shifts from the major-type to the brain type transcript by switching from the major-type promoter to the brain type promoter. The neuronal enhancer instead of the major enhancer may work on the brain type promoter, depending on DNA methylation in CGI2. The maternally active major-type promoter becomes silent without transcription factors, and consequently, the Eed/Ezh2 PcG complex binds to make the chromatin structure silent. This implies that the PcG complex is necessary to maintain cell-type-specific imprinting. It remains unknown how neuron-specific imprinting is regulated by DNA methylation and/or histone modifications mediated by the PcG complex, because *Dnmt3L*$^{m-/-}$ and *Eed*$^{-/-}$ embryos are lethal by E10.5 (4, 14) and E8.5 (11), respectively, just before neurogenesis.

As far as we know, this is the first report of an epigenetic analysis of cultured cells where DNA methylation and chromatin remodeling by PcG proteins establish and maintain cell-type-specific imprinting at one gene locus. Although allelic DNA methylation established in the gamete contributes primarily to tissue-specific imprinting, tissue-specific *Grb10* imprinting is directly regulated by the repressive chromatin mediated by the PcG complex during development. Our analysis of promoter-specific and cell-type-specific imprinting of *Grb10* gives an important clue for understanding the mechanism of tissue-specific imprinting.

ACKNOWLEDGMENTS

We thank F. Ishino for providing information about genomic sequences of *Grb10* promoter regions.

T.K. was supported in part by a Grant-in-Aid for Scientific Research (C) and a Grant-in-Aid on Priority Areas (Molecular Brain Science) from the Ministry of Education, Culture, Sports, Science and Technology of Japan.

REFERENCES

1. **Arnaud, P., D. Monk, M. P. Hichins, E. Gordon, W. Dean, C. Beechey, J. Peters, W. Craigen, M. Preece, P. Stanier, G. E. Moore, and G. Kelsey.** 2003. Conserved methylation imprints in the human and mouse GRB10 genes with divergent allelic expression suggests differential reading of the same mark. Hum. Mol. Genet. **12:**1005–1019.
2. **Arnaud, P., K. Hata, M. Kaneda, E. Li, H. Sasaki, R. Feil, and G. Kelsey.** 2006. Stochastic imprinting in the progeny of Dnmt3L−/− females. Hum. Mol. Genet. **15:**589–598.
3. **Bantignies, F., and G. Cavalli.** 2006. Cellular memory and dynamic regulation of Polycomb group proteins. Curr. Opin. Cell Biol. **18:**1–9.
4. **Bourc'his, D., G. L. Xu, C. S. Lin, B. Bollman, and T. H. Bester.** 2001. Dnmt3L and the establishment of maternal genomic imprints. Science **294:** 2536–2539.
5. **Cao, R., L. Wang, H. Wang, L. Xia, H. Erdjument-Bromage, P. Tempst, R. S. Jones, and Y. Zhang.** 2002. Role of histone H3 lysine 27 methylation in Polycomb-group silencing. Science **298:**1039–1043.
6. **Cattanach, B. M., and C. V. Beechey.** 1990. Autosomal and X-chromosome imprinting. Dev. Suppl. **1990:**63–72.
7. **Constancia, M., B. Pickard, G. Kelsey, and W. Reik.** 1988. Imprinting mechanisms. Genome Res. **8:**881–900.
8. **Czermin, B., R. Melfi, D. McCabe, V. Seitz, A. Imhof, and V. Pirrotta.** 2002. Drosophila enhancer of Zeste/ESC complexes have a histone H3 methyltransferase activity that marks chromosomal Polycomb sites. Cell **111:**185–196.
9. **Davies, W., A. R. Isles, and L. S. Wilkinson.** 2005. Imprinted gene expression in the brain. Neurosci. Biobehav. Rev. **29:**421–430.
10. **Esumi, S., N. Kakazu, Y. Taguchi, T. Hirayama, A. Sasaki, T. Hirabayashi, T. Koide, T. Kitsukawa, S. Hamada, and T. Yagi.** 2005. Monoallelic yet combinatorial expression of variable exons of the protocadherin-α gene cluster in single neurons. Nat. Genet. **37:**171–176.
11. **Faust, C., A. Schumacher, B. Holdener, and T. Magnuson.** 1995. The eed mutation disrupts anterior mesoderm production in mice. Development **121:** 273–285.
12. **Fournier, C., Y. Goto, E. Ballestar, K. Delaval, A. M. Hever, M. Esteller, and R. Feil.** 2002. Allele-specific histone lysine methylation marks regulatory regions at imprinted mouse genes. EMBO J. **21:**6560–6570.
13. **Gregory, R. I., T. E. Randall, C. A. Johnson, S. Khosla, I. Hatada, L. P. O'Neill, B. M. Turner, and R. Feil.** 2001. DNA methylation is linked to deacethylation of histone H3, but not H4, on the imprinted genes *Snrpn* and *U2af1-rs1*. Mol. Cell. Biol. **21:**5426–5436.
14. **Hata, K., M. Okano, H. Lei, and E. Li.** 2002. Dnmt3L cooperates with the Dnmt3 family of de novo DNA methyltransferases to establish maternal imprints in mice. Development **129:**1983–1993.
15. **Higashimoto, K., H. Soejima, H. Yatsuki, K. Joh, M. Uchiyama, Y. Obata, R. Ono, Y. Wang, Z. Xin, X. Zhu, S. Masuko, F. Ishino, I. Hatada, Y. Jinno, T. Iwasaka, T. Katsuki, and T. Mukai.** 2002. Characterization and imprinting status of *OBPH1/Obph1* gene: implications for an extended imprinting domain in human and mouse. Genomics **80:**575–584.
16. **Higashimoto, K., T. Urano, K. Sugiura, H. Yatsuki, K. Joh, W. Zhao, M. Iwakawa, H. Ohashi, M. Oshimura, N. Niikawa, T. Mukai, and H. Soejima.** 2003. Loss of CpG methylation is strongly correlated with loss of histone H3 lysine 9 methylation at DMR-LIT1 in patients with Beckwith-Wiedemann syndrome. Am. J. Hum. Genet. **73:**948–956.
17. **Hikichi, T., T. Kohda, T. Kaneko-Ishino, and F. Ishino.** 2003. Imprinting regulation of the murine *Meg1/Grb10* and human *GRB10* genes; roles of brain-specific promoters and mouse-specific CTCF-binding sites. Nucleic Acids Res. **31:**1398–1406.
18. **Kaneda, M., M. Okano, K. Hata, T. Sado, N. Tsujimoto, E. Li, and H. Sasaki.** 2004. Essential role for de novo DNA methyltransferase Dnmt3a in paternal and maternal imprinting. Nature **429:**900–903.
19. **Kishino, T.** 2006. Imprinting in neurons. Cytogenet. Genome Res. **113:**209–214.
20. **Kuzmichev, A., K. Nishioka, H. Erdjument-Bromage, P. Tempst, and D. Reinberg.** 2002. Histone methyltransferase activity associated with a human multiprotein complex containing the Enhancer of Zeste protein. Genes Dev. **16:**2893–2905.
21. **Lau, J. C., M. L. Hanel, and R. Wevrick.** 2004. Tissue-specific and imprinted epigenetic modifications of the human *NDN* gene. Nucleic Acids Res. **32:** 3376–3382.
22. **Lewis, A., K. Mitsuya, D. Umlauf, P. Smith, W. Dean, J. Walter, M. Higgins, R. Feil, and W. Reik.** 2004. Imprinting on distal chromosome 7 in the placenta involves repressive histone methylation independent of DNA methylation. Nat. Genet. **36:**1291–1295.
23. **Li, T., T. H. Vu, G. A. Ulaner, Y. Yang, J. F. Hu, and A. R. Hoffman.** 2004. Activating and silencing histone modifications from independent allelic switch regions in the imprinted *Gnas* gene. Hum. Mol. Genet. **13:**741–750.
24. **Mager, J., N. D. Montgomery, F. P. de Villena, and T. Magnuson.** 2003. Genome imprinting regulated by the mouse Polycomb group protein Eed. Nat. Genet. **33:**502–507.
25. **Muller, J., C. M. Hart, N. J. Francis, M. L. Vargas, A. Sengupta, B. Wild, E. L. Miller, M. B. O'Connor, R. E. Kingston, and J. A. Simon.** 2002. Histone methyltransferase activity of a Drosophila Polycomb group repressor complex. Cell **111:**197–208.
26. **Nakagawachi, T., H. Soejima, T. Urano, W. Zhao, K. Higashimoto, Y. Satoh, S. Matsukura, S. Kudo, Y. Kitajima, H. Harada, K. Furukawa, H. Matsuzaki, M. Emi, Y. Nakabeppu, K. Miyazaki, M. Sekiguchi, and T. Mukai.** 2003. Silencing effect of CpG island hypermethylation and histone modifications on O6-methylguanine-DNA methyltransferase (*MGMT*) gene expression in human cancer. Oncogene **22:**8835–8844.
27. **Pirrotta, V.** 1995. Chromatin complexes regulating gene expression in Drosophila. Curr. Opin. Genet. Dev. **5:**466–472.
28. **Rougeulle, C., P. Navarro, and P. Avner.** 2003. Promoter-restricted H3 Lys 4 di-methylation is an epigenetic mark for monoallelic expression. Hum. Mol. Genet. **12:**3343–3348.
29. **Saitoh, S., and T. Wada.** 2000. Parent-of-origin specific histone acetylation and reactivation of a key imprinted gene locus in Prader-Willi syndrome. Am. J. Hum. Genet. **66:**1958–1962.
30. **Surani, M. A., S. C. Barton, and M. L. Norris.** 1984. Development of reconstituted mouse eggs suggests imprinting of the genome during gametogenesis. Nature **308:**548–550.
31. **Tilghman, S. M.** 1999. The sins of the fathers and mothers: genomic imprinting in mammalian development. Cell **96:**185–193.
32. **Uejima, H., M. P. Lee, H. Cui, and A. P. Feinberg.** 2000. Hot-stop PCR: a simple and general assay for linear quantitation of allele ratios. Nat. Genet. **25:**375–376.
33. **Umlauf, D., Y. Goto, R. Cao, F. Cerqueira, A. Wagschal, Y. Zhang, and R. Feil.** 2004. Imprinting along the *Kcnq1* domain on mouse chromosome 7 involves repressive histone methylation and recruitment of Polycomb group complexes. Nat. Genet. **36:**1296–1300.
34. **van der Vlag, J., and A. P. Otte.** 1999. Transcriptional repression mediated by the human polycomb-group protein EED involves histone deacetylation. Nat. Genet. **23:**474–478.
35. **Vu, T. H., T. Li, and A. R. Hoffman.** 2004. Promoter-restricted histone code,

not the differentially methylated DNA regions or antisense transcripts, marks the imprinting status of *IGF2R* in human and mouse. Hum. Mol. Genet. **13:**2233–2245.

36. **Wang, J., J. Mager, Y. Chen, E. Schneider, J. C. Cross, A. Nagy, and T. Magnuson.** 2001. Imprinted X inactivation maintained by a mouse Polycomb group gene. Nat. Genet. **28:**371–375.
37. **Wang, Y., K. Joh, S. Masuko, H. Yatsuki, H. Soejima, A. Nabetani, C. V. Beechey, S. Okinami, and T. Mukai.** 2004. The mouse *Murr1* gene is imprinted in the adult brain, presumably due to transcriptional interference by the antisense-oriented *U2af1-rs1* gene. Mol. Cell. Biol. **124:**270–279.
38. **Yamasaki, K., K. Joh, T. Ohta, H. Masuzaki, T. Ishimaru, T. Mukai, N. Niikawa, M. Ogawa, J. Wagstaff, and T. Kishino.** 2003. Neurons but not glial cells show reciprocal imprinting of sense and antisense transcripts of *Ube3a*. Hum. Mol. Genet. **12:**837–847.
39. **Yamasaki, Y., T. Kayashima, H. Soejima, A. Kinoshita, K. Yoshiura, N. Matsumoto, T. Ohta, T. Urano, H. Masuzaki, T. Ishimaru, T. Mukai, N. Niikawa, and T. Kishino.** 2005. Neuron-specific relaxation of *Igf2r* imprinting is associated with neuron-specific histone modifications and lack of its antisense transcript *Air*. Hum. Mol. Genet. **14:**2511–2520.
40. **Yang, Y., T. Li, T. H. Vu, G. A. Ulaner, J. F. Hu, and A. R. Hoffman.** 2003. The histone code regulating expression of the imprinted mouse *Igf2r* gene. Endocrinology **144:**5658–5670.

Human Pathology (2007) 38, 621–628

ELSEVIER

Human
PATHOLOGY

www.elsevier.com/locate/humpath

Original contribution

RET oncogene amplification in thyroid cancer: correlations with radiation-associated and high-grade malignancy☆

Masahiro Nakashima MD[a,*], Noboru Takamura MD[e], Hiroyuki Namba MD[b], Vladimir Saenko PhD[c], Serik Meirmanov MD[a], Naomichi Matsumoto MD[d,h], Tomayoshi Hayashi MD[f], Shigeto Maeda MD[g], Ichiro Sekine MD[a]

[a]*Tissue and Histopathology Section, Division of Scientific Data Registry, Atomic Bomb Disease Institute, Nagasaki University Graduate School of Biomedical Sciences, Nagasaki 852-8523, Japan*
[b]*Department of Molecular Medicine, Atomic Bomb Disease Institute, Nagasaki University Graduate School of Biomedical Sciences, Nagasaki 852-8523, Japan*
[c]*Department of International Health and Radiation Research, Atomic Bomb Disease Institute, Nagasaki University Graduate School of Biomedical Sciences, Nagasaki 852-8523, Japan*
[d]*Department of Human Genetics, Atomic Bomb Disease Institute, Nagasaki University Graduate School of Biomedical Sciences, Nagasaki 852-8523, Japan*
[e]*Department of Public Health, Nagasaki University Graduate School of Biomedical Sciences, Nagasaki 852-8523, Japan*
[f]*Department of Pathology, Nagasaki University Hospital, Nagasaki 852-8501, Japan*
[g]*Department of Surgery, Nagasaki University Hospital, Nagasaki 852-8501, Japan*
[h]*Department of Human Genetics, Yokohama City University Graduate School of Medicine, Yokohama 236-0004, Japan*

Received 25 August 2006; revised 12 October 2006; accepted 12 October 2006

Keywords:
Thyroid cancer;
RET amplification;
Radiation;
FISH;
Genomic instability

Summary A radiation etiology is well known in thyroid carcinogenesis. *RET* oncogene rearrangement is the most common oncogenic alteration in Chernobyl-related papillary thyroid cancer (PTC). To find the characteristic alteration associated with *RET* rearrangements in radiation-induced thyroid cancers, we analyzed the *RET* oncogene by fluorescence in situ hybridization. The fluorescence in situ hybridization technique has the possibility of detecting *RET* rearrangements at a single-cell level regardless of the specific fusion partner involved and directly reveals *RET* copy number on a per-cell basis. Our study demonstrated *RET* amplification in all 3 cases of radiation-associated thyroid cancers but not in sporadic well-differentiated PTC (n = 11). Furthermore, *RET* amplification was observed in all 6 cases of sporadic anaplastic thyroid cancers (ATCs). The frequency of *RET* amplification-positive cells was higher in ATC (7.2%-24.1%) than in PTC (1.5%-2.7%). The highest frequency of *RET* amplification-positive cells was observed among ATC cases with a strong p53 immunoreactivity. In conclusion, we found *RET* amplification, which is a rare oncogenic aberration, in thyroid cancer. This report is the first

☆ This work was supported in part through Nagasaki University 21st Century Center of Excellence (COE) program and by Grant for Research Project of Atomic Bomb Diseases from the Japanese Ministry of Health, Labour and Welfare.

* Corresponding author. Tissue and Histopathology Section, Division of Scientific Data Registry, Atomic Bomb Disease Institute, Nagasaki University Graduate School of Biomedical Sciences, Nagasaki 852-8523, Japan.
E-mail address: moemoe@nagasaki-u.ac.jp (M. Nakashima).

0046-8177/$ – see front matter
doi:10.1016/j.humpath.2006.10.013

one to suggest the presence of *RET* amplification in PTC and ATC. *RET* amplification was correlated with radiation-associated, high-grade malignant potency, and p53 accumulation, suggesting genomic instability. *RET* amplification might be induced by a high level of genomic instability in connection with progression of thyroid carcinogenesis and, subsequently, be associated with radiation-induced and/or high-grade malignant cases.

1. Introduction

The incidence of papillary thyroid cancer (PTC) was reported to be elevated in both atomic-bomb survivors in Hiroshima and Nagasaki, Japan, and residents living in areas exposed to fallout from the Chernobyl accident, suggesting a radiation etiology in thyroid carcinogenesis. *RET* rearrangement is a well-known molecular alteration observed in PTC. Ret oncoproteins, which function as receptor tyrosine kinases, are dimerized by ligand-binding, activated, and subsequently involved in regulating cell growth and survival in normal tissues [1,2]. During thyroid carcinogenesis, if the 3′ -end of *RET* oncogenes rearrange with other genes containing a coiled-coil domain, they dimerize without ligand stimuli and constitutively activate cell growth and survival in thyroid follicular cells, finally promoting the occurrence of PTC [3-5].

To date, at least 15 different variants of *RET* rearrangement have been reported [6]. *RET* rearrangements are the most common oncogenic alterations in Chernobyl-related PTC; 4 large studies have found that 50% to 90% of Chernobyl-related PTC show *RET* rearrangements—nearly all of them to *RET/PTC1* or *RET/PTC3* [7-10]—resulting from paracentric inversion of chromosome 10 [11]. Although *RET/PTC1* and *RET/PTC3* are most often found in sporadic cases of PTC, their prevalence may vary within a broad range, from 0% to more than 60% [6]. Other less common variants, usually formed as a result of interchromosomal translocation, occur in an extremely limited number of cases. Most often, such translocations have been found in radiation-induced PTC [12]. However, specific molecular alterations have not been identified in radiation-induced PTC.

In the present study, to find the characteristic/specific alterations in *RET* rearrangements in radiation-induced thyroid cancers, we analyzed the *RET* oncogene by fluorescence in situ hybridization (FISH) on paraffin-embedded tissues. Previous studies using FISH analysis of *RET* rearrangements have demonstrated its utility in thyroid cancers [13,14]. The FISH technique can detect *RET* rearrangements at a single-cell level regardless of the specific fusion partner involved and directly reveals *RET* copy number on a per-cell basis.

Here, we describe the presence of *RET* oncogene amplification, which is a rare type of *RET* cytogenetic alteration in PTC. Oncogene amplification is extremely common in human tumors. In thyroid cancers, *RET* oncogene amplification correlated with radiation-induced, high-grade malignancy and anaplastic transformation of PTC. To our knowledge, this is the first report demonstrat-

Table 1 Clinicopathologic profiles of patients and summary of results

Case	Age	Sex	Px	pTNM	Radiation	*RET* rearrangement	*RET* amplification		p53
							Positive cells	Copy no.[a]	
1	32	F	FV	T1N0M0	Tx	Δrfp/ret[b]	1.5%	5.6 (4-8)	-
2	41	F	FV	T4N1bM0	C	PTC3	2.7%	4.8 (3-9)	-
3P	44	M	WD	T1N0M0	-	-	-		-
3R	57	M	ATC	T4N0M0	Tx	-	24.1%	5.2 (3-8)	+
4	64	M	ATC	T3N0M0	-	-	20.3%	6.3 (4-10)	+
5	77	F	ATC	T4N0M0	-	-	19.5%	6.6 (4-8)	+
6	71	F	ATC	T4N1bM0	-	-	13.1%	5.8 (3-8)	-
7	84	F	ATC	T4N0M0	-	-	7.2%	4.8 (3-6)	-
8	78	M	ATC	T4N0M0	-	-	8.9%	5.6 (4-7)	-
9	81	F	ATC	T2N0M0	-	-	10.2%	6.1 (3-7)	-
10	22	F	PD	T4N1aM0	-	PTC1	2.4%	4.5 (4-6)	-
Others (n = 10)	52[c]	F/M (8:2)	WD	T1N0M0	-	-	-		-

Abbreviations: M, male; F, female; Px, pathologic diagnosis; FV, follicular variant PTC; WD, well-differentiated PTC; PD, poorly differentiated PTC; Tx, irradiation therapy; C, Chernobyl case; P, primary; R, recurrent (after irradiation therapy).

[a] Values are shown as mean (range).

[b] Ref [16].

[c] Mean age.

Table 2 List of primers and PCR conditions

Target	Sequence	Annealing (°C)	Amplicon (bp)
RET/PTC1			
Forward	GCCTGGAGGAGCTCACCAA	56	255
Reverse	CTCTGCCTTTCAGATGGAA		
RET/PTC3			
Forward	ACCTGCCAGTGGTTATCAAGCT	58	154
Reverse	TTCGCCTTCTCCTAGAGTTTTTCC		
α-Tubulin			
Forward	AGATCATTGACCTCGTGTTGGA	56	101
Reverse	ACCAGTTCCCCCACCAAAG		

ing *RET* amplification in PTC and anaplastic thyroid cancers (ATC), although *RET* amplification has been reported in medullary thyroid cancer cases [15].

2. Materials and methods

2.1. Subjects

All samples were formalin-fixed paraffin-embedded tissues. The sections were used for FISH analysis and RNA preparation. Three cases of radiation-associated thyroid cancers including 2 cases of PTC and 1 case of anaplastic thyroid cancer (ATC) were explored for *RET* rearrangement by dual-color interphase FISH and reverse transcriptase–polymerase chain reaction (RT-PCR). The clinicopathologic profiles of the 3 radiation-associated cases were as follows: Case 1: a 32-year-old Russian woman received surgical treatment for thyroid cancer that was histologically diagnosed as a follicular variant of PTC. Four years before the surgery, the patient had undergone

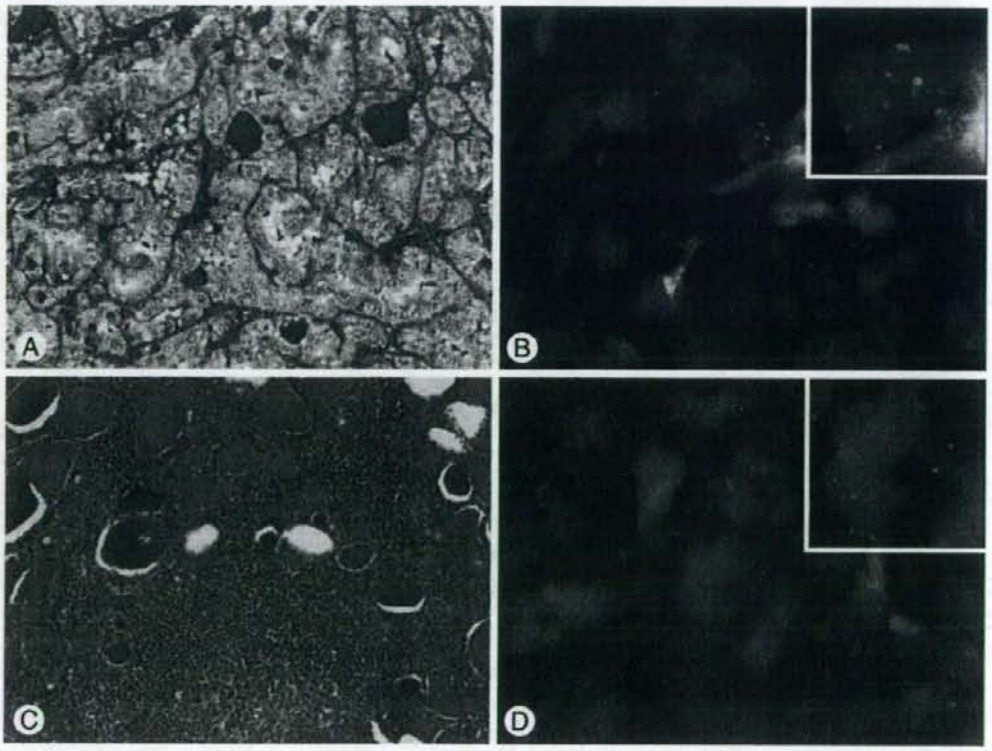

Fig. 1 A case (case 1) of radiation-induced papillary carcinoma, follicular variant (A). FISH analysis demonstrates cancer cells showing 2 *CEP10* and several randomly distributed *RET* signals, suggesting *RET* gene amplification (B). In the nontumor area (C), infiltrating lymphocytes and follicular cells show 2 *RET* signals coupled with 2 *CEP10* signals, suggesting a wild-type *RET* (D).

external radiation therapy (40 Gy) for primary mediastinal lymphoma. A novel tumorigenic rearrangement, *Δrfp/ret*, which was a translocation between chromosomes 6 and 10, was identified as shown in our previous report [16]. Case 2: the patient was a 41-year-old Russian woman living in a radioactively contaminated area around the Chernobyl-accident site; she was 25 years old at the time of the accident and was operated on under the diagnosis of thyroid cancer. A histologic examination revealed it as a follicular variant of PTC. Case 3: a 44-year-old Japanese man was operated on under the diagnosis of thyroid cancer and treated by internal radiation with ^{131}I after the operation. He died of tumor recurrence at 57 years of age. The pathologic diagnosis of the primary cancer was "well differentiated PTC" and that of the recurrent tumor was "ATC." None of these radiation-associated cases received chemotherapy.

As a control in this study, 10 cases of sporadic PTC and 6 cases of sporadic ATC, which had no histories of exposure to atomic bombing, radiation therapy, or chemotherapy, were also analyzed. The clinicopathologic profiles of the patients are summarized in Table 1. The experimental protocol was approved by the Ethics Review Committee of Nagasaki University Graduate School of Biomedical Sciences (Protocol No. 0305150036-2).

2.2. Dual-color interphase FISH

For hybridization, 1 μg DNA of BAC clone RP11-351D16 (accession number AC010864, human chromosome 10q11 containing the *RET* locus) was directly labeled with SpectrumGreen-dUTP by using Nick Translation Kit (Vysis Inc, Downers Grove, Ill) according to the manufacturer's instructions. Deparaffinized sections were heated by microwave in a 0.01 mol/L citrate buffer (pH 6.0) and pretreated with 0.3% pepsin. Subsequently, slides were immersed in 0.1% NP-40 and denatured by heating in 70% formamide/2×SSC. The mixture containing the above-mentioned DNA probes and SpectrumOrange-labeled DNA probes corresponding to the centromere of chromosome 10 (*CEP10*, Vysis Inc) was denatured and applied to the denatured tissue. The slides were covered with a coverslip, sealed with rubber

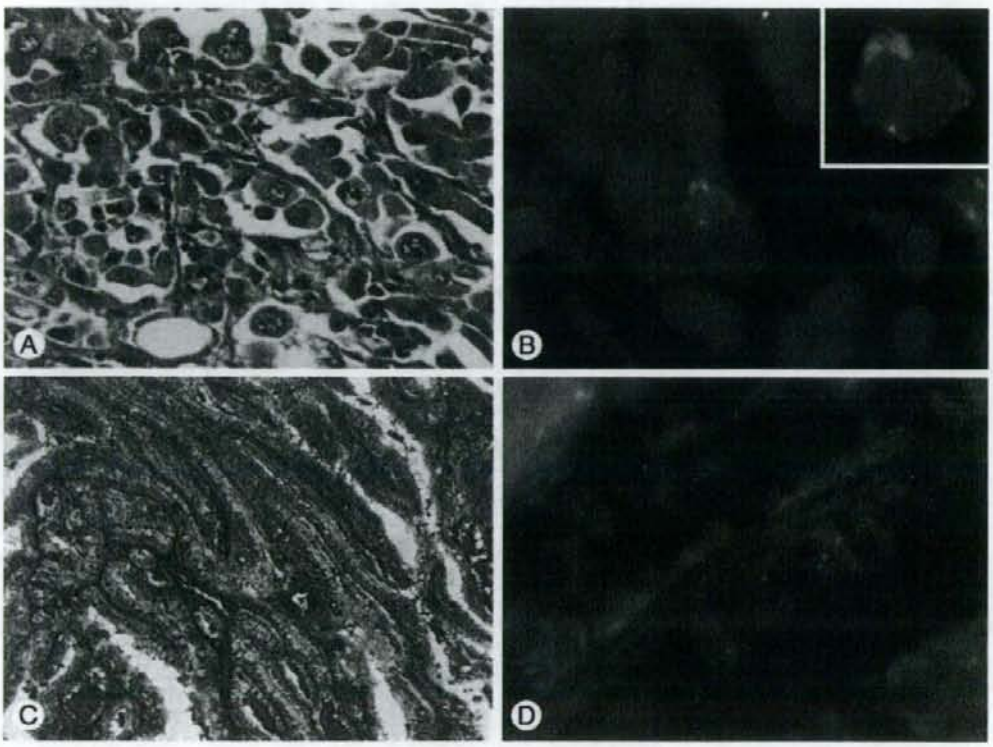

Fig. 2 A case (case 3R) of recurrent anaplastic carcinoma induced by radiation therapy of the primary thyroid tumor (A). FISH analysis demonstrates *RET* amplification in cancer cells (B). The histologic type of the primary tumor (case 3P) was that of a well-differentiated papillary carcinoma (C). A wild type of *RET* signals is evident in this primary cancer (D).

cement, and incubated for 16 hours at 42°C in a humidified chamber. After hybridization, slides were washed, then counterstained and visualized with 4′,6-diamidino-2-phenylindole dihydrochloride (Vysis Inc), and photographed using a fluorescence microscope (Zeiss Axioplan2, Carl Zeiss Japan, Tokyo, Japan) equipped with a CCD camera, and then analyzed with IPLab/MAC image software (Scanalytics Inc, Fairfax, Va). Signals were analyzed in up to 20 viewing areas per case at the 1000-fold magnification.

2.3. Reverse transcriptase–polymerase chain reaction

Total RNA was isolated from tissues with High Pure RNA Paraffin Kit (Roche, Mannheim, Germany) according to the manufacturer's protocol and examined for *RET/PTC1* and *RET/PTC3*. Expressions of *RET/PTC1*, *RET/PTC3*, and *α-tubulin* genes were assessed by RT-PCR using the respective primers designed with the Primer Express Software (PE Applied Biosystems, Foster City, Calif). All reactions were performed with the SuperScript One-Step RT-PCR with Platinum *Taq* System (Invitrogen, Carlsbad, Calif) according to the manufacturer's protocol. Primer sequences, annealing temperature settings in the PCR reactions, and size of amplicons are listed in Table 2.

2.4. Immunohistochemistry

After immersion in 0.3% H_2O_2/methanol, sections were preincubated with 10% normal goat serum. After antigen retrieval, tissues were incubated overnight at 4°C with anti-p53 monoclonal antibody (DO-7, DakoCytomation, Glostrup, Denmark) at a 1:50 dilution. The slides were subsequently incubated with biotinylated goat antimouse IgG antibody for 1 hour, followed by incubation with avidin-peroxidase, and visualized with diaminobenzidine.

3. Results

3.1. Fluorescence in situ hybridization analysis

All results are summarized in Table 1. The FISH analysis for *RET* gene demonstrated nuclei exhibiting several (up to 10) green signals and 2 orange signals in thyroid cancer cells, suggesting amplification of the *RET* gene. All 3 radiation-associated cases—cases 1 (Fig. 1), 2, and 3R (Fig. 2)—showed *RET* amplification, regardless of histologic type and tumor grade; case 1 was a low-grade (pT1N0M0) and case 2 a high-grade (pT4N1bM0) follicular variant of PTC, whereas case 3R was a high-grade (pT4N0M0) ATC. *RET* amplification was also found in all 6 cases of sporadic ATC. On the other hand, in 10 cases of non–radiation-associated PTC, *RET* amplification was evident in only 1 case (case 10; Fig. 3), which was a poorly differentiated and high-grade (pT4N1aM0) PTC from a 22-year-old Japanese woman, whereas the others were of the classical type and low-grade (pT1N0M0) PTC. Although there was no significant difference in the number of extracopies of the gene between cases, the frequency of *RET* amplification-positive cells was higher in ATC (mean, 14.8%; range, 7.2%-24.1%) than in PTC (mean, 2.2%; range, 1.5%-2.7%). The highest frequency of *RET* amplification-positive cells was observed in ATC cases with a strong p53 immunoreactivity (Fig. 4). No *RET* amplification was observed in case 3P (Fig. 2). No *RET* amplification was identified by FISH in normal thyroid follicles surrounding tumors in any of the cases.

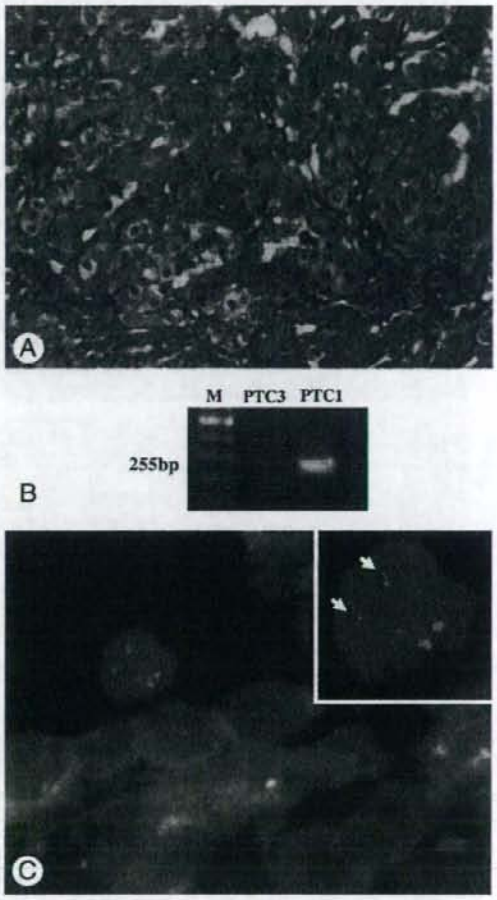

Fig. 3 A case (case 10) of high-grade poorly differentiated carcinoma with no history of radiation exposure (A). RT-PCR reveals *RET/PTC1* rearrangement in this case (B). FISH analysis demonstrates *RET* amplification in cancer cells (C). Two signals in the proximity of the homologous centromere are also observed, suggesting a paracentric inversion of *RET/PTC* rearrangements in the same nuclei (arrows in C).

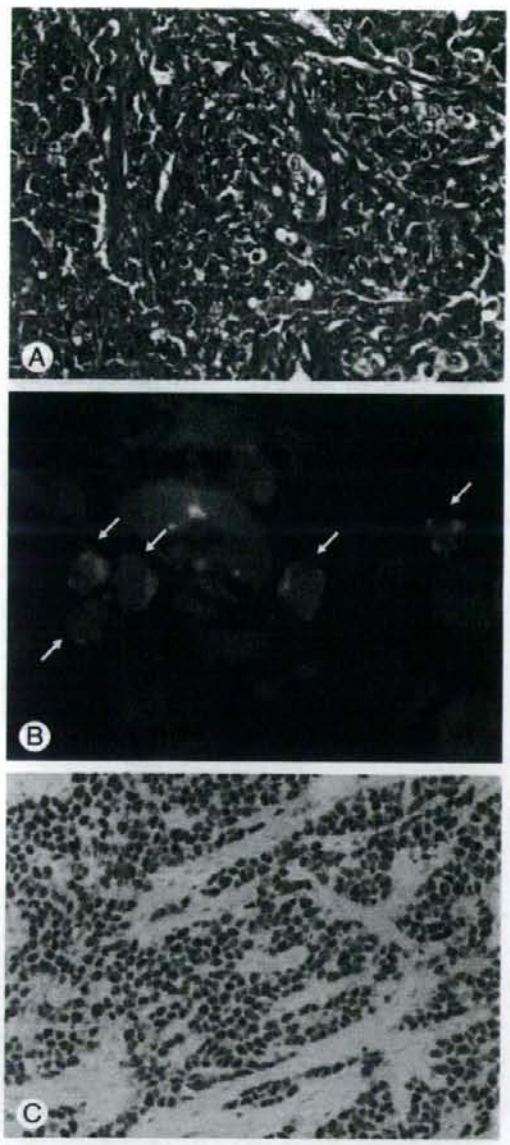

Fig. 4 A case (case 4) of anaplastic carcinoma with no history of radiation exposure (A). In this case, FISH analysis demonstrates several cancer cells showing *RET* amplification (arrows) in a high-power field (B). Immunostaining reveals diffuse and intense p53 immunoreactivity, suggesting an accumulation of mutated p53 proteins (C).

3.2. RT-PCR analysis

RT-PCR analyses revealed *RET/PTC1* and *RET/PTC3* in cases 2 and 10 (Fig. 3C), respectively. Neither *RET/PTC1* nor *RET/PTC3* was demonstrated in other PTC cases or in any ATC cases (data not shown). These results are summarized in Table 1.

3.3. P53 expression

Immunohistochemical results for p53 expression are also shown in Table 1. Intense and diffuse p53 immunoreactivity was evident in the nuclei of cancer cells in 3 cases of ATC, including both a radiation-associated case (case 3R) and 2 sporadic cases (cases 4 and 5), but not in any of the PTC cases. All of the p53-positive ATC cases showed a high frequency (mean, 21.3%; range, 19.5%-24.1%) of *RET* amplification-positive cells (Fig. 4).

4. Discussion

Gene amplification is a term used to indicate the production of multiple copies of a specific gene [17]; it is associated with genomic instability, the main characteristic of cancer cells, and it frequently involves proto-oncogenes [18]. Oncogenes are often amplified in advanced solid tumors, and the amplification correlates with a poor prognosis for patients with ovarian cancer (*HER-2/neu*), breast cancer (*C-MYC, HER-2/neu*), neuroblastoma (*N-MYC*), or small cell lung cancer (*C-MYC*) [19-22]. We found *RET* oncogene amplification in thyroid cancers in vivo. In PTC, *RET* amplification was found in radiation-associated and high-grade cases. Because *RET* amplification was not observed in sporadic, well-differentiated, and low-grade cases of PTC, *RET* amplification could be a molecular marker for radiation-induced and/or high-grade PTC. Furthermore, *RET* amplification was frequently observed in ATC regardless of whether it was a radiation-associated or a sporadic case. In case 3, *RET* amplification was only found in recurrent cancer with anaplastic transformation after irradiation therapy but not in the primary tumor, which was a conventional type PTC. Thus, *RET* amplification may be associated with anaplastic transformation during thyroid tumorigenesis.

Anaplastic thyroid cancer has been reported to arise from preexisting differentiated thyroid cancer [23,24]. In thyroid carcinogenesis, mutations of the *P53* gene are involved in anaplastic and poorly differentiated thyroid carcinomas but not in well-differentiated PTC [25,26]. The cell cycle checkpoint function of wild-type p53 maintains genomic stability and ploidy. Therefore, loss of wild-type p53 functions may be associated with genomic instability—manifested as a complex karyotype during anaplastic transformation—after DNA-damaging chemotherapy and radiation. In our cases, the highest frequency of *RET* amplification-positive cells was observed in ATC cases showing a diffuse p53 overexpression, which included a case of anaplastic transformation after irradiation therapy. These findings suggest that *RET* amplification may be induced by a high level of genomic instability due to *P53* mutation. Interestingly, other authors have also reported

correlations between *P53* aberrations and oncogene amplifications in other solid tumors, such as esophageal, ovarian, bladder, and colorectal cancers [27-30].

Amplification of oncogenes leads to the overexpression of proteins participating in the transduction of growth-related signals and confers a growth advantage to tumor cells during carcinogenesis [31,32]. In such tumors, a majority of cancer cells should express oncogene amplification, suggesting a clonal oncogenesis. However, in our results, *RET* amplification-positive cells were restricted to only a small proportion (1.5%-24.1%) of cells and were never clustering in thyroid cancers. Therefore, we suggest that *RET* amplification is not directly involved in thyroid carcinogenesis, but is rather a randomly induced subclonal event in cancer cells due to a high level of genomic instability associated with progression of cancer stages, which results in intratumoral heterogeneity. A distinct intratumoral heterogeneity has previously been reported for many solid tumors [33-35], suggesting that clonal evolution in such tumors is more complex than predicted by linear models [36]. Similarly, Unger et al [14] have found a heterogeneity in the distribution of *RET* rearrangements in PTC with interphase FISH and have suggested that RET protein does play a role in the generation of tumor, perhaps through paracrine interaction with *RET* rearrangement-negative cells. Furthermore, Zhang et al [37] have demonstrated low-level amplifications of oncogenes, such as *TERT*, *C-MYC*, *CCND1*, and *ERBB2*, which contribute to the development and progression of tumors through different pathways and are frequently detected in cervical cancers. A combination of these amplifications often occurred in different proportions in advanced tumors [37]. Thus, *RET* amplification might play a role in advanced thyroid cancer cooperatively with other oncogenes. Further analyses, such as studies on the expression of the RET protein or mRNA, are required to confirm the oncogenic role of *RET* amplification during thyroid carcinogenesis.

In conclusion, we found *RET* amplification, which is a rare cytogenetic aberration, in thyroid cancer. To the best of our knowledge, this report is the first one to suggest the presence of *RET* oncogene amplification in thyroid cancers other than medullary carcinoma. *RET* amplification was correlated with radiation-associated, high-grade malignant potency and p53 accumulation, suggesting genomic instability. *RET* amplification might be induced by a high level of genomic instability connected with progression of thyroid carcinogenesis and, subsequently, be associated with radiation-induced and/or high-grade malignant cases.

Acknowledgment

The authors are grateful to Prof. Tahara of the Radiation Effects Research Foundation for valuable comments in this study.

Appendix A. Supplementary data

Supplementary data associated with this article can be found, in the online version, at doi:10.1016/j.humpath.2006.10.013.

References

[1] Takahashi M, Buma Y, Iwamoto T, Inaguma Y, Ikeda H, Hiai H. Cloning and expression of the ret proto-oncogene encoding a tyrosine kinase with two potential transmembrane domains. Oncogene 1988; 3:571-8.

[2] Schuchardt A, D'Agati V, Larsson-Blomberg L, Costantini F, Pachnis V. Defects in the kidney and enteric nervous system of mice lacking the tyrosine kinase receptor Ret. Nature 1994;367:380-3.

[3] Grieco M, Santoro M, Berlingieri MT, et al. PTC is a novel rearranged form of the ret proto-oncogene and is frequently detected in vivo in human thyroid papillary carcinomas. Cell 1990;60:557-63.

[4] Jhiang SM, Sagartz JE, Tong Q, et al. Targeted expression of the ret/PTC1 oncogene induces papillary thyroid carcinomas. Endocrinology 1996;137:375-8.

[5] Powell Jr DJ, Russell J, Nibu K, et al. The RET/PTC3 oncogene: metastatic solid-type papillary carcinomas in murine thyroids. Cancer Res 1998;58:5523-8.

[6] Tallini G, Asa SL. RET oncogene activation in papillary thyroid carcinoma. Adv Anat Pathol 2001;8:345-54.

[7] Nikiforov YE, Rowland JM, Bove KE, Monforte-Munoz H, Fagin JA. Distinct pattern of RET oncogene rearrangements in morphological variants of radiation induced and sporadic papillary carcinomas in children. Cancer Res 1997;57:1690-4.

[8] Thomas GA, Bunnell H, Cook HA, et al. High prevalence of RET/PTC rearrangements in Ukrainian and Belarussian post-Chernobyl thyroid papillary carcinomas: a strong correlation between RET/PTC3 and the solid-follicular variant. J Clin Endocrinol Metab 1999; 84:4232-8.

[9] Santoro M, Thomas GA, Vecchio G, et al. Gene rearrangement and Chernobyl related thyroid cancers. Br J Cancer 2000;82:315-22.

[10] Rabes HM, Demidchik EP, Sidorow JD, et al. Pattern of radiation-induced RET and NTRK1 rearrangements in 191 post-Chernobyl papillary carcinomas: biological, phenotypic, and clinical implications. Clin Cancer Res 2000;6:1093-103.

[11] Jhiang SM. The RET proto-oncogene in human cancers. Oncogene 2000;19:5590-7.

[12] Williams D. Cancer after nuclear fallout: lessons from the Chernobyl accident. Nat Rev Cancer 2002;2:543-9.

[13] Corvi R, Martinez-Alfaro M, Harach HR, Zini M, Papotti M, Romeo G. Frequent RET rearrangements in thyroid papillary microcarcinoma detected by interphase fluorescence in situ hybridization. Lab Invest 2001;81:1639-45.

[14] Unger K, Zitzelsberger H, Salvatore G, et al. Heterogeneity in the distribution of RET/PTC rearrangements within individual post-Chernobyl papillary thyroid carcinomas. J Clin Endocrinol Metab 2004;89:4272-9.

[15] Huang SC, Torres-Cruz J, Pack SD, et al. Amplification and overexpression of mutant RET in multiple endocrine neoplasia type 2-associated medullary thyroid carcinoma. J Clin Endocrinol Metab 2003;88:459-63.

[16] Saenko V, Rogounovitch T, Shimizu-Yoshida Y, et al. Novel tumorigenic rearrangement, Δrfp/ret, in a papillary thyroid carcinoma from externally irradiated patient. Mutat Res 2003;527: 81-90.

[17] Brown DD, Dawid IB. Specific gene amplification in oocytes. Oocyte nuclei contain extrachromosomal replicas of the genes for ribosomal RNA. Science 1968;60:272-80.

[18] Zimonjic DB, Zhang H, Shan Z, et al. DNA amplification associated with double minutes originating from chromosome 19 in mouse hepatocellular carcinoma. Cytogenet Cell Genet 2001;93:114-6.
[19] Slamon DJ, Clark GM, Wong SG, Levin WJ, Ullrich A, McGuire WL. Human breast cancer: correlation of relapse and survival with amplification of the HER-2/neu oncogene. Science 1987;235: 177-82.
[20] Slamon DJ, Godolphin W, Jones LA, et al. Studies of the HER-2/neu proto-oncogene in human breast and ovarian cancer. Science 1989; 244:707-12.
[21] Seeger RC, Brodeur GM, Satjer H, et al. Association of multiple copies of the N-myc oncogene with rapid progression of neuroblastomas. N Engl J Med 1985;313:1111-6.
[22] Johnson BE, Battey J, Linnoila I, et al. Changes in the phenotype of human small cell lung cancer cell lines after transfection and expression of the c-myc proto-oncogene. J Clin Invest 1986;78: 525-32.
[23] Nishiyama RH, Dunn EL, Thompson NW. Anaplastic spindle-cell and giant-cell tumors of the thyroid gland. Cancer 1972;30:113-27.
[24] Aldinger KA, Samaan NA, Ibanez M, Hill Jr CS. Anaplastic carcinoma of the thyroid: a review of 84 cases of spindle and giant cell carcinoma of the thyroid. Cancer 1978;41:2267-75.
[25] Ito T, Seyama T, Mizuno T, et al. Unique association of p53 mutations with undifferentiated but not with differentiated carcinomas of the thyroid gland. Cancer Res 1992;52:1369-71.
[26] Donghi R, Longoni A, Pilotti S, Michieli P, Della Porta G, Pierotti MA. Gene p53 mutations are restricted to poorly differentiated and undifferentiated carcinomas of the thyroid gland. J Clin Invest 1993;91:1753-60.
[27] Persons DL, Croughan WS, Borelli KA, Cherian R. Interphase cytogenetics of esophageal adenocarcinoma and precursor lesions. Cancer Genet Cytogenet 1998;106:11-7.
[28] Wang ZR, Liu W, Smith ST, Parrish RS, Young SR. c-Myc and chromosome 8 centromere studies of ovarian cancer by interphase FISH. Exp Mol Pathol 1999;66:140-8.
[29] Mahdy E, Pan Y, Wang N, Malmstrom PU, Ekman P, Bergerheim U. Chromosome 8 numerical aberration and C-MYC copy number gain in bladder cancer are linked to stage and grade. Anticancer Res 2001;21:3167-73.
[30] Ozakyol A, Ozdemir M, Artan S. Fish detected p53 deletion and N-MYC amplification in colorectal cancer. Hepatogastroenterology 2006;53:192-5.
[31] Stark GR, Debatisse M, Giulotto E, Wahl GM. Recent progress in understanding mechanisms of mammalian DNA amplification. Cell 1989;57:901-8.
[32] Snapka RM. Gene amplification as a target for cancer chemotherapy. Oncol Res 1992;4:145-50.
[33] Walch AK, Zitzelsberger HF, Bruch J, et al. Chromosomal imbalances in Barrett's adenocarcinoma and the metaplasia-dysplasia-carcinoma sequence. Am J Pathol 2000;156:555-66.
[34] Aubele M, Malttis A, Zitzelsberger H, et al. Intratumoral heterogeneity in breast carcinoma revealed by laser-microdissection and comparative genomic hybridization. Cancer Genet Cytogenet 1999;110:94-102.
[35] Zitzelberger H, Kulka U, Lehmann L, et al. Genetic heterogeneity in a prostatic carcinoma and associated prostatic intraepithelial neoplasia as demonstrated by combined use of laser-microdissection, degenerate oligonucleotide primed PCR and comparative genomic hybridization. Virchows Arch 1998;433:297-304.
[36] Barrett MT, Sanchez CA, Prevo LJ, et al. Evolution of neoplastic cell lineages in Barrett esophagus. Nat Genet 1999;22:106-9.
[37] Zhang A, Månér S, Betz R, et al. Genetic alterations in cervical carcinomas: frequent low-level amplifications of oncogenes are associated with human papilloma virus infection. Int J Cancer 2002; 101:427-33.

American Journal of Medical Genetics Part A 143A:546–552 (2007)

Congenital Arhinia:
Molecular-Genetic Analysis of Five Patients

Daisuke Sato,[1,2,3] Osamu Shimokawa,[1,3,4] Naoki Harada,[3,4] Oystein E. Olsen,[5] Jia-Woei Hou,[6] Wolfgang Muhlbauer,[7] Ellen Blinkenberg,[8] Nobuhiko Okamoto,[9] Akira Kinoshita,[1] Naomichi Matsumoto,[3,10] Shinji Kondo,[3,11] Tatsuya Kishino,[3,11] Nobutomo Miwa,[1,3] Tadashi Ariga,[2] Norio Niikawa,[1,3] and Koh-ichiro Yoshiura[1,3]*

[1]Department of Human Genetics, Nagasaki University Graduate School of Biomedical Sciences, Nagasaki, Japan
[2]Department of Pediatrics, Hokkaido University Graduate School of Medicine, Sapporo, Japan
[3]Solution Oriented Research of Science and Technology (SORST), Japan Science and Technology Agency (JST), Kawaguchi, Japan
[4]Kyushu Medical Science, Nagasaki, Japan
[5]Department of Radiology, Great Ormond Street Hospital for Children, London, UK
[6]Division of Medical Genetics, Department of Pediatrics, Chang Gung Children's Hospital, Taoyuan, Taiwan
[7]Plastic Surgery Arabella, Munich, Germany
[8]Center for Medical Genetics and Molecular Medicine, Haukeland University Hospital, Bergen, Norway
[9]Department of Planning and Research, Osaka Medical Center and Research Institute for Maternal and Child Health, Izumi, Japan
[10]Department of Human Genetics, Yokohama City Graduate School of Medicine, Yokohama, Japan
[11]Division of Functional Genomics, Center for Frontier Life Sciences, Nagasaki University, Nagasaki, Japan

Received 30 May 2006; Accepted 30 October 2006

Congenital arhinia, complete absence of the nose, is an extremely rare anomaly with unknown cause. To our knowledge, a total of 36 cases have been reported, but there has been no molecular-genetic study on this anomaly. We encountered a sporadic case of congenital arhinia associated with a de novo chromosomal translocation, t(3;12)(q13.2;p11.2). This led us to analyze the patient by BAC-based FISH for translocation breakpoints and whole-genome array CGH for other possible deletions/duplications in the genome. We found in this patient an approximately 19 Mb deletion spanning from 3q11.2 to 3q13.31 but no disruption of any gene(s) at the other breakpoint, 12p11.2. As the deleted segment at 3q was a strong candidate region containing the putative arhinia gene, we also performed the array CGH in four other arhinia patients with normal karyotypes, as well as mutation analysis of two genes, *COL8A1* and *CPOX*, selected among hundreds of genes located to the deleted region, because they are expressed during early stages of human craniofacial development. However, in the four patients, there were no copy number aberrations in the region examined or no mutations in the two genes. Although our study failed to identify the putative arhinia gene, the data may become a clue to unravel the underlying mechanism of arhinia. © 2007 Wiley-Liss, Inc.

Key words: arhinia; translocation breakpoint; deletion; 3q; 12p; FISH; array CGH

How to cite this article: Sato D, Shimokawa O, Harada N, Olsen OE, Hou J-W, Muhlbauer W, Blinkenberg E, Okamoto N, Kinoshita A, Matsumoto N, Kondo S, Kishino T, Miwa N, Ariga T, Niikawa N, Yoshiura K-i. 2007. Congenital arhinia: Molecular-genetic analysis of five patients. Am J Med Genet Part A 143A:546–552.

INTRODUCTION

Congenital arhinia, complete absence of the nose, is an extremely rare abnormality with unknown cause. Congenital arhinia is often associated with microphthalmia, choanal atresia, and/or cleft palate [Graham and Lee, 2006]. To the best of our knowledge, only 36 cases of arhinia have been reported [Ruprecht and Majewski, 1978; Kaminker et al., 1985; Cohen and Goitein, 1986; Sakai et al., 1989; Galetti et al., 1994; Onizuka et al., 1995; Thiele et al., 1996;

Grant sponsor: Grants-in-Aid for Scientific Research; Grant number: 13854024; Grant sponsor: Applied Genomics; Grant numbers: 17019055, 17590288; Grant sponsor: Ministry of Education, Culture, Sports, Science and Technology (MEXT) of Japan; Grant sponsor: SORST (Japan Science and Technology Agency, JST).

*Correspondence to: Koh-ichiro Yoshiura, MD, PhD, Department of Human Genetics, Nagasaki University Graduate School of Biomedical Sciences, Sakamoto 1-12-4, Nagasaki 852-8523, Japan.
E-mail: kyoshi@net.nagasaki-u.ac.jp

DOI 10.1002/ajmg.a.31613

Choi et al., 1998; Cusick et al., 2000; Olsen et al., 2001; McGlone, 2003; Hou, 2004; Jules et al., 2004; Mathur et al., 2005; Shino et al., 2005; Graham and Lee, 2006]. Most cases were sporadic, but two familial cases were also reported [Ruprecht and Majewski, 1978; Thiele et al., 1996]. As two sisters with arhinia and microphthalmia were born to non-consanguineous parents, an autosomal recessive mode of inheritance has been suggested in this family [Ruprecht and Majewski, 1978]. In the other family, an aunt and a niece were affected with arhinia, suggesting a dominant mode of inheritance with reduced penetrance [Thiele et al., 1996]. Of the 17 patients who were karyotyped, 14 had a normal karyotype, whereas three cases had 46,XX/47,XX,+9 [Kaminker et al., 1985], inv(9) [Cohen and Goitein, 1986], or t(3;12)(q13.2;p11.2) [Hou, 2004]. These findings may indicate that genetic factors play a role in the occurrence of arhinia. Several genes have been proposed as candidates for arhinia, such as *PAX6* and its downstream targets, those of the FGF signaling, *MSX1*, *NRP2*, *GSC*, *ALX3*, and *ALX4* [Hou, 2004; Graham and Lee, 2006]. However, no genetic analysis has yet been undertaken. A de novo balanced reciprocal chromosomal translocation with a congenital disorder provides a good opportunity to discover the gene causing the disease [Mizuguchi et al., 2004].

We previously encountered a patient with congenital arhinia, small eyes and other abnormalities who was cytogenetically diagnosed to have a translocation, t(3;12)(q13.2;p11.2) [Hou, 2004]. Under a hypothesis that a gene responsible for arhinia is disrupted at either of the breakpoints of the translocation, we performed breakpoint analysis of the patient as well as genome analyses of four other patients with arhinia.

MATERIALS AND METHODS

Subjects

This study was approved by the Committee for Ethical Issues on Human Genome and Gene Analysis, Nagasaki University. Five patients with arhinia were collected and analyzed as a collaboration study among six medical institutions (Nagasaki University Graduate School of Biomedical Sciences, Nagasaki, Japan; Great Ormond Street Hospital for Children, London, UK; Chang Gung Children's Hospital, Taoyuan, Taiwan; Plastic Surgery Arabella, Munich, Germany; Center for Medical Genetics and Molecular Medicine, Haukeland University Hospital, Bergen, Norway; and Osaka Medical Center and Research Institute for Maternal and Child Health, Osaka, Japan). Clinical findings of these five patients are shown in Table I. One patient (Patient A) had a de novo translocation, t(3;12)(q13.2;p11.2) and the other four patients (Patients B–E) were karyotypically normal.

We first focused our interest on Patient A and carried out a breakpoint analysis to try to isolate the

TABLE I. Clinical Findings of Five Patients With Arhinia

	Patients [References]				
	A	B	C	D	E
Clinical findings	[Hou, 2004]	[Okamoto, unpublished]	[Muhlbauer et al., 1993]	[Olsen et al., 2001]	[Sakai et al., 1989]
Sex	F	M	F	F	M
Karyotype	46,XX,t(3;12)(q13.2;p11.2)	46,XY	46,XX	46,XX	46,XY
High arched palate	+	+	+	+	+
Hypertelorism	+	+	+	+	+ (pseudo)
Microphthalmia	Bilateral	Left	NA	NA	–
Coloboma iris	+	Left	NA	Bilateral	–
Published					
Development	NA	N	N	N	N
Brain imaging	N	N	N	N	N
Olfactory bulbs	–	–	NA	–	NA
Family history	–	–	–	–	–
Pregnancy	UN	UN	UN	PH	NA
Birth weight (g)	2,800	2,368	2,640	3,070	3,346
Paranasal sinuses	UD	+	–	–	NA
Nasolacrimal ducts	NA	–	–	–	–
Complications	Scoliosis, epilepsy	Hypogonadism, autism	–	–	–
Current status	Living DD GR	Living	Living ND GR NNB	Unknown	Living

F, female; M, male; +, observed; –, not observed; NA, not assessed; N, normal; UN, uneventful; PH, polyhydramnios; UD, underdeveloped; DD, delayed development; ND, normal development; GR, growth retardation; NNB, no nasal breathing.

FIG. 1. Patient B at age 6 days, showing the absence of the nose.

putative arhinia gene. Detailed clinical features of Patients A, C, D, and E were reported previously [Sakai et al., 1989; Muhlbauer et al., 1993; Olsen et al., 2001; Hou, 2004, respectively]. Patient B was a Japanese boy whose clinical manifestations have been unpublished. He was born to healthy and non-consanguineous parents by cesarean at 39 weeks of gestation with a birth weight of 2,368 g, length 48 cm, and OFC of 33.7 cm (Fig. 1). Because of his congenital arhinia, a nasal airway was created by a surgical operation at age 17 days to facilitate oral feeding. Other clinical manifestations included bilateral microphthalmia, coloboma of the iris, mid-face hypoplasia, high arched palate, hypertelorism, and absent nasolacrimal ducts. He had neither cleft palate nor low set ears. At age 4 years, his weight was 12.7 kg, height 94.7 cm, and OFC 50 cm, and had paranasal sinuses, normal hearing acuity, autistic behavior, and hypogonadotropic hypogonadism. He is currently able to eat foods through his mouth by himself. His psychomotor developmental quotient was estimated at 65.

Fluorescence In Situ Hybridization (FISH) Analysis

Metaphase chromosomes were prepared from an immortalized lymphoblastoid cell line according to the standard protocol [Shimokawa et al., 2005]. The RPCI-11 human BAC clones mapped around the breakpoints, 3q13.2 and 12p11.2, were selected and used for FISH analyses. Mapping information was retrieved from the UCSC genome browser, 2003 July version (http://genome.ucsc.edu/cgi-bin/hgGateway). BAC-clone DNA was extracted using an automatic DNA extraction system (Kurabo, Osaka, Japan) and labeled with SpectrumGreen-11-dUTP or SpectrumOrange-11-dUTP (Vysis, Downers Grove, IL) by nick translation. Fluorescent probes were hybridized to metaphase chromosomes for 16–72 hr, and then chromosome slides were washed and counterstained with DAPI using standard protocols [Shimokawa et al., 2005]. Fluorescence signals were observed under Zeiss Axioskop microscope equipped with a quad filter set with single-band excitation filters (84000, Chroma Technology Corporation, Brattleboro, VT). Images were captured by cooled CCD camera (TEA/CCD-1317-G1, Princeton Instruments, Trenton, NJ) and merged with IPLab/MA.

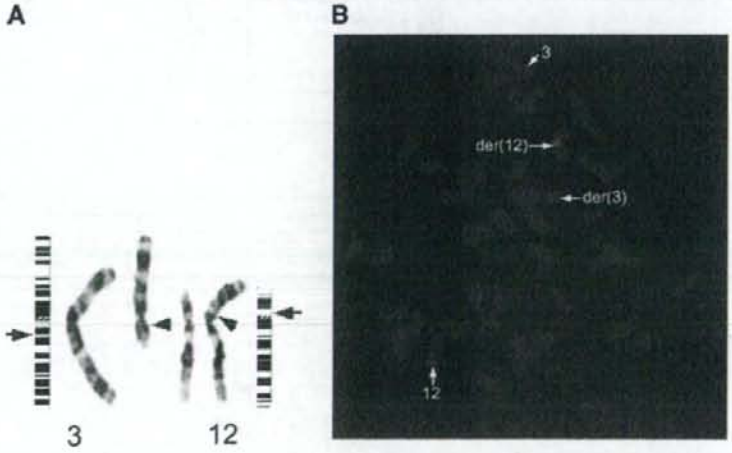

FIG. 2. A: Partial karyotype of Patient A. Arrows and arrowheads show the breakpoints. B: FISH analysis in Patient A. Green signals for a BAC clone, RP11-55L17, that spans the 12p breakpoint appear on der(3), der(12) and normal chromosome 12, while red signals for a chromosome 3-derived clone, RP11-803P6, are seen only on normal chromosome 3. The findings indicate a deletion only in der(3).

Array Comparative Genomic Hybridization (CGH)

DNA was extracted from peripheral blood lymphocytes by conventional method [Sambrook and Russell, 2001]. To detect chromosomal aberrations, we performed homemade whole-genome BAC-based array CGH (array CGH) using genomic DNA of all five patients according to the method described previously [Miyake et al., 2006]. The microarray contains 2,173 BAC and PAC clones which span the whole genome at each of 1.5 Mb average.

Mutation Analysis

A screening for mutations of *COL8A1* and *CPOX* was performed in the four arhinia patients with normal karyotypes. All exon sequences and their flanking intron sequences of the two genes were amplified by PCR for direct sequencing. PCR conditions were set at 40 cycles of 94°C for 30 sec, 62°C for 30 sec, and 72°C for 45 sec in a 15 μl mixture containing 1 × PCR buffer with 1.5 mM $MgCl_2$, 0.2 mM each of dNTP, 1 μM each primer and 0.4 Units Taq polymerase (TaKaRa, Otsu, Japan). PCR products were treated with ExoSAP-IT (Amersham Biosciences, Piscateway, NJ) and both strands were sequenced with BigDye Terminator Sequencing kit version 3.1 according to the supplied protocol (Applied Biosystems, Foster City, CA). The reaction mixture was purified using Sephadex G-50 superfine (Amersham Biosciences) and analyzed on the ABI Genetic Analyzer 3100 (Applied Biosystems) with the Sequence Analysis software (Applied Biosystems) and aligned with the Auto Assembler version2.1.1 software (Applied Biosystems) to find DNA alterations.

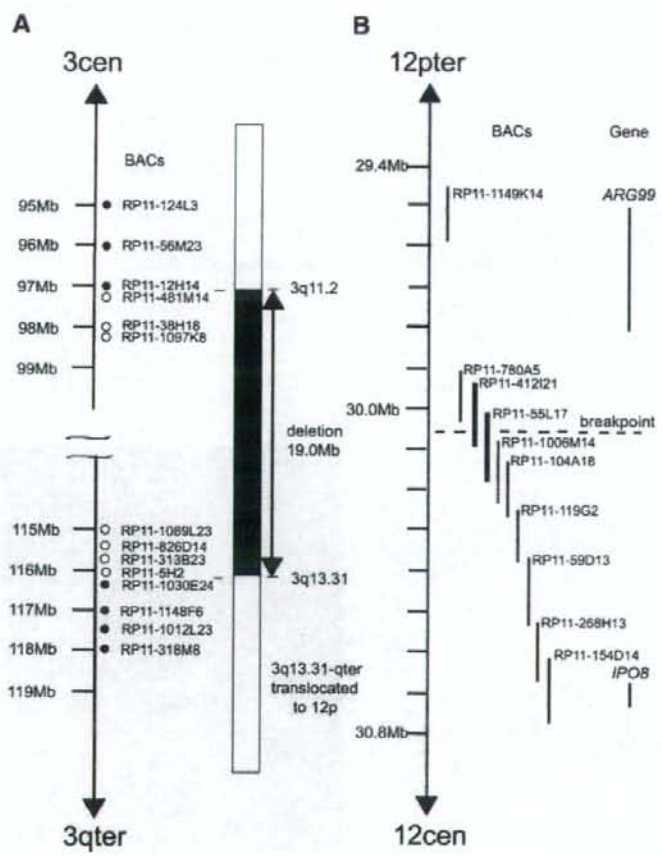

FIG. 3. **A**: Physical map covering the 3q11.2–3q13.31 deleted region of Patient A. Solid and open circles indicate the presence and absence of clones in Patient A, respectively. **B**: Physical map of the 12p11 breakpoint region. Thick lines indicate BAC clones covering the breakpoint. Genes *ARG99* and *IPO8* are located close to the breakpoint.

RESULTS AND DISCUSSION

Although the translocation of Patient A looked balanced (Fig. 2A) [Hou, 2004], there was actually a relatively large deletion at the 3q13.2 breakpoint region of her derivative chromosome 3. FISH analysis revealed that the 3q proximal end of the deleted segment was confined to 3q11.2 between BAC clones, RP11-12H14, and RP11-481M14, and the distal end to 3q13.31 between RP11-5H2 and RP11-1030E24 (Figs. 2B and 3). Since lacking signals were confirmed for 16 other BACs that are located between the two ends, the deletion extended to approximately 19 Mb in size from 3q11.2 to 3q13.31 (UCSC Genome Browser). As for the other derivative chromosome 12, as two neighbor BAC clones, RP11-412I21, and RP11-55L17, in a contig were identified to cover the 12p11.22 breakpoint, there was no deletion at the breakpoint.

To know whether any other chromosomal aberrations exist in the genome of the five patients examined, whole-genome array CGH was performed. Consequently, the array CGH confirmed in Patient A the presence of the 3q deletion (Fig. 4) without deletions or duplications in any other chromosomes. In Patient D, four regions were suspected to have duplication, but this could not be confirmed by subsequent FISH, because her chromosome preparation was not available. There was no chromosomal aberration in the remaining three patients.

A literature search for deletions for 3q11.2–3q13.31 found eight reported cases [Arai et al., 1982; Jenkins et al., 1985; McMorrow et al., 1986; Okada et al., 1987; Fujita et al., 1992; Genuardi et al., 1994; Ogilvie et al., 1998]. The smallest region of overlap (SRO) for deletion among them is almost confined to 3q12–3q13.31 (Fig. 5). The deletion in one patient (Case 8 in Fig. 5) [Jenkins et al., 1985] was reported to lie between 3q11 and 3q21. However, the exact location of the proximal border in this patient was not clear since either FISH or molecular analysis was not carried out. None but one patient [Arai et al., 1982] had any nose anomaly, and none of the eight patients manifested microphathalmia that is virtually accompanied with arhinia [Graham and Lee, 2006]. The exceptional patient whose deletion involved 3q13–q21 (Case 7, Fig. 5) had alobar holoprosencephaly, arhinia, and cleft lip [Arai et al., 1982]. Although arhinia of this case seems atypical and to be a holoprosencephaly-associated median facial anomaly, the patient might provide possible information for localization of the arhinia locus. If the locus exists at the long arm of chromosome 3, it might be confined to a segment between 3q11.2 and the proximal border of the deletion of Case 8

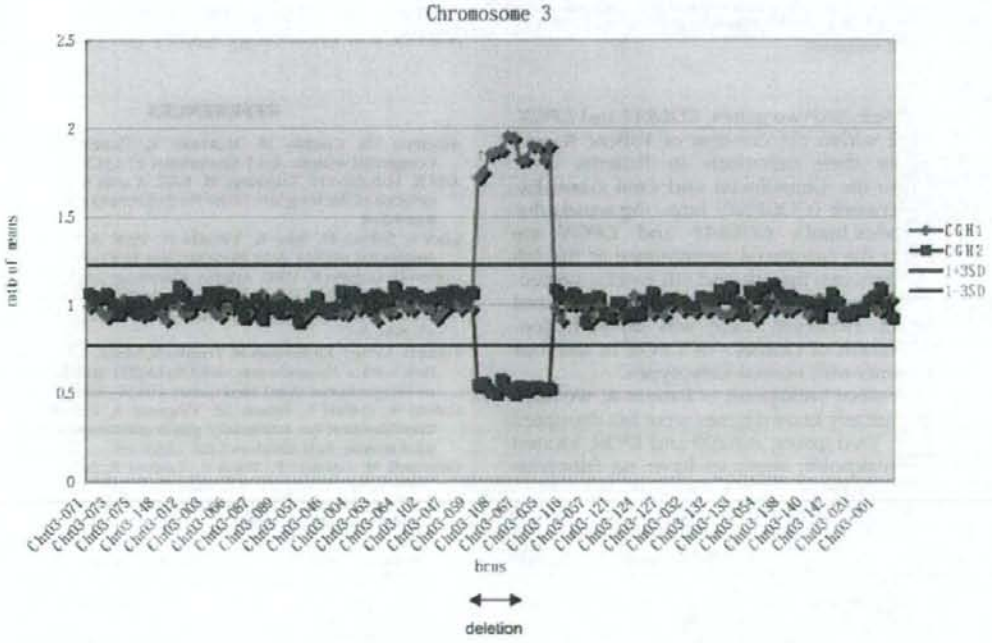

FIG. 4. Array CGH analysis in Patient A, showing a deletion on 3q. The clone at the proximal end within the deletion was RP11-262O19 (3q11.2), and the distal end clone was RP11-342J15 (3q13.31), the results suggesting that the deletion is approximately 18 Mb in size.

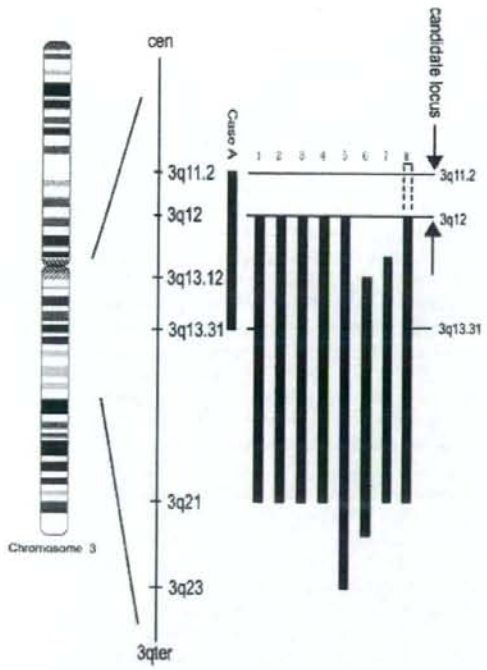

FIG. 5. Extent (bars) of 3q11.2–3q13.31 deletion in Patient A and eight reported cases. **Lanes 1–8** are from McMorrow et al. [1986], Ogilvie et al. [1998], Okada et al. [1987], Fujita et al. [1992], Genuardi et al. [1994], Arai et al. [1982], and Jenkins et al. [1985], respectively.

(Fig. 5). We selected two genes, *COL8A1* and *CPOX*, from 3q11.2 within the deletion of Patient A, and analyzed for their mutations in Patients B–E. According to the Craniofacial and Oral Gene Expression Network (COGENE, http://hg.wustl.edu/COGENE/index.html), *COL8A1* and *CPOX* are expressed in the frontnasal prominence at the 4th week, and between the 4th and 5th weeks, respectively, suggesting they play some roles in the nasal development. However, there was no pathogenomonic mutation of *COL8A1* or *CPOX* in the four arhinia patients with normal karyotypes.

As for the other breakpoint of Patient A, we have confirmed that any known genes were not disrupted at 12p11.22. Two genes, *ARG99* and *IPO8*, located near the breakpoint, seem to have no functions related to the human nasal development. However, it cannot totally be ruled out that there may be unknown RNA transcript(s) on the breakpoint or the breakage may affect a long-distance position effect [Velagaleti et al., 2005].

The nasal placode, the anlage of the nose, begins to develop from the 12th to the 13th Carnegie stage, at the end of the fourth embryonic week. The stage between the end of the 4th week to the 7th week is the most active, important period in the human nose development [O'Rahilly, 1967; Kim et al., 2004]. A failure of the developmental process may result in arhinia, for example, failure of growth or overgrowth of the medial and lateral nasal process sequentially leads to premature fusion of the medial nasal processes [Albernaz et al., 1996].

In conclusion, analysis of five patients with arhinia revealed, although a 19 Mb large deletion involving 3q11–q13 was identified in one patient, no chromosome aberrations or gene mutations were found in the other four patients. Nevertheless, our findings may become a clue to isolate the putative arhinia gene. Further molecular studies in new patients, as well as that on other genes within the deleted region in Patient A, are needed to unravel the underlying cause of arhinia. This is the first report of molecular-genetic study on congenital arhinia.

ACKNOWLEDGMENTS

Participation of all patients in this study is highly appreciated. We also thank Ms Y. Noguchi, K. Miyazaki and A. Goto for their technical assistance. This study was supported by Grants-in-Aid for Scientific Research (Category S, No. 13854024 and Priority Areas—Applied Genomics, No. 17019055 for N. N.; and No. 17590288 for K. Y.) from the Ministry of Education, Culture, Sports, Science and Technology (MEXT) of Japan, and by SORST from the Japan Science and Technology Agency (JST) for N. N.

REFERENCES

Albernaz VS, Castillo M, Mukherji K, Ihmeidan IH. 1996. Congenital arhinia. Am J Neuroradiol 17:1312–1314.

Arai K, Matukiyo H, Takazawa H. 1982. A case report of partial deletion of the long arm of the No.3 chromosome. Med Genet Res 4:1–4.

Choi S, Shiozu H, Sato K, Nishida H. 1998. A case report of congenital arhinia. Acta Neonatol Jpn 34:83–86.

Cohen D, Goitein K. 1986. Arhinia. Rhinology 24:287–292.

Cusick W, Sullivan CA, Rojas B, Poole AE, Poole DA. 2000. Prenatal diagnosis of total arhinia. Ultrasound Obstet Gynecol 15:259–261.

Fujita H, Meng J, Kawamura M, Tozuka N, Ishii F, Tanaka N. 1992. Boy with a chromosome del(3)(q12q23) and blepharophimosis syndrome. Am J Med Genet 44:434–436.

Galetti R, Dallari S, Bruzzi M, Vincenzi A, Galetti G. 1994. Consideration on respiratory physiopathology in a case of total arhinia. Acta Otorhinol Ital 14:63–69.

Genuardi M, Calvieri F, Tozzi C, Coslovi R, Neri G. 1994. A new case of interstitial deletion of chromosome 3q,del(3q)(q13.12q21.3), with agenesis of the corpus callosum. Clin Dysmorphol 3:292–296.

Graham JM, Lee J. 2006. Bosma arhinia microphthalmia syndrome. Am J Med Genet Part A 140A:189–193.

Hou JW. 2004. Congenital arhinia with de novo reciprocal translocation, t(3;12)(q13.2;p11.2). Am J Med Genet Part A 130A:200–203.

Jenkins MB, Stang HJ, Davis E, Boyd L. 1985. Deletion of the proximal long arm of chromosome 3 in an infant with features of Turner syndrome. Ann Génét (Paris) 28:42–44.

Jules AF, Cynthia MG, Terry T, Samue S, Brian S, Larry H. 2004. Vertical facial distraction in the treatment of arhinia. Plast Reconstr Surg 113:2061–2066.

Kaminker CP, Dain L, Lamas MA, Sanchez JM. 1985. Mosaic trisomy 9 syndrome with unusual phenotype. Am J Med Genet 22:237–241.

Kim CH, Park HW, Kim K, Yoon JH. 2004. Early development of the nose in human embryos: A stereomicroscopic and histologic analysis. Laryngoscope 114:1791–1800.

Mathur NN, Dubey NK, Kumar S, Bothra R, Chadha A. 2005. Arhinia. Int J Pediatr Otorhinolaryngol 69:97–99.

McGlone L. 2003. Congenital arhinia. J Paediatr Child health 39:474–476.

McMorrow LE, Reid CS, Coleman J, Medeiros A, D'Andrea M, Santucci T, McCormack MK. 1986. A new interstitial deletion of the long arm of chromosome 3. Am J Hum Genet 39: A124.

Miyake N, Shimokawa O, Harada N, Sosonkina N, Okubo A, Kawara H, Okamoto N, Ohashi H, Kurosawa K, Naritomi K, Kaname T, Nagai T, Shotelersuk V, Hou JW, Fukushima Y, Kondoh T, Matsumoto T, Shinoki T, Kato M, Tonoki H, Nomura M, Yoshiura K, Kishino T, Ohta T, Niikawa N, Matsumoto N. 2006. No detectable genomic aberrations by BAC array CGH in Kabuki make-up syndrome patients. Am J Med Genet Part A 140A:291–293.

Mizuguchi T, Collod-Beroud G, Akiyama T, Harada N, Morisaki T, Abifadel M, Allard D, Varret M, Claustres M, Ihara M, Kinoshita A, Yoshiura K, Junien C, Kajii T, Jondeau G, Niikawa N, Boileau C, Matsumoto N. 2004. Heterozygous *TGFBR2* mutations in Marfan syndrome. Nat Genet 36:855–860.

Muhlbauer W, Schmidt A, Fairley J. 1993. Simultaneous construction of an internal and external nose in an infant with arhinia. Plast Reconstr Surg 91:720–725.

O'Rahilly R. 1967. The early development of the nasal pit in staged human embryos. Anat Rec 157:380.

Ogilvie CM, Rooney SC, Hodgson SV, Berry AC. 1998. Deletion of chromosome 3q proximal region gives rise to a variable phenotype. Clin Genet 53:220–222.

Okada N, Hasegawa T, Osawa M, Fukuyama Y. 1987. A case of de novo interstitial deletion 3q. J Med Genet 24:305–308.

Olsen OE, Gjelland K, Reigstad H, Rosendahl K. 2001. Congenital absence of the nose: A case report and literature review. Pediatr Radiol 31:225–232.

Onizuka T, Ohkubo F, Hosaka Y, Ichinose M, Keiko Okazaki K. 1995. Arhinia: A case report. Worldplast 1:65–71.

Ruprecht KW, Majewski F. 1978. Familial arhinia combined with Peter's anomaly and maxillar deformities, a new malformation syndrome? Klin Mbl Augenheilk 172:708–715.

Sakai Y, Ohara Y, Inoue Y. 1989. Congenital complete absence of the nose. J Jpn Plast Reconstr Surg 9:265–273.

Sambrook J, Russell DW. 2001. Molecular cloning: A laboratory manual. Cold Spring Harbor, New York: Cold Spring Harbor Laboratory Press.

Shimokawa O, Miyake N, Yoshimura T, Sosonkina N, Harada N, Mizuguchi T, Kondoh S, Kishino T, Ohta T, Remco V, Takashima T, Kinoshita A, Yoshiura K, Niikawa N, Matsumoto N. 2005. Molecular characterization of del(8)(p23.1p23.1) in a case of congenital diaphragmatic hernia. Am J Med Genet Part A 136A:49–51.

Shino M, Chikamatsu K, Yasuoka Y, Nagai K, Furuya N. 2005. Congenital arhinia: A case report and functional evaluation. Laryngoscope 115:1118–1123.

Thiele H, Musil A, Nagel F, Majewski F. 1996. Familial arhinia, choanal atresia, and microphthalmia. Am J Med Genet 63:310–313.

Velagaleti GVN, Bien-Willner GA, Northup JK, Lockhart LH, Hawkins JC, Jalal SM, Withers M, Lupski JR, Stankiewicz P. 2005. Position Effects due to chromosome breakpoints that map ~900 kb upstream and ~1.3 Mb downstream od SOX9 in two patients with Campomelic dysplasia. Am J Hum Genet 76:652–662.